IN SITU GROUNDWATER ARSENIC REMOVAL USING IRON OXIDE-COATED SAND

A Thesis

by

HONGXU YU

Submitted to the Office of Graduate Studies of
Texas A&M University
in partial fulfillment of the requirements for the degree of

MASTER OF SCIENCE

August 2010

Major Subject: Biological and Agricultural Engineering

In Situ Groundwater Arsenic Removal Using Iron Oxide-Coated Sand

IN SITU GROUNDWATER ARSENIC REMOVAL

USING IRON OXIDE-COATED SAND

A Thesis

by

HONGXU YU

Submitted to the Office of Graduate Studies of
Texas A&M University
in partial fulfillment of the requirements for the degree of

MASTER OF SCIENCE

Approved by:

Chair of Committee,	Yongheng Huang
Committee Members,	Youjun Deng
	Raghupathy Karthikeyan
Head of Department,	Gerald Riskowski

August 2010

Major Subject: Biological and Agricultural Engineering

ABSTRACT

In Situ Groundwater Arsenic Removal Using Iron Oxide-Coated Sand. (August 2010)

Hongxu Yu, B.A., Tsinghua University;

M.S., Tsinghua University

Chair of Advisory Committee: Dr. Yongheng Huang

In many regions of the world, groundwater is contaminated with a high level of arsenic that must be treated before it can be safely used as drinking water. *In situ* immobilization of arsenic from groundwater within subsurface environment could have major advantages over the conventional above-ground chemical coagulation-precipitation treatment process. In this study, we develop a novel technique that can *in situ* emplace iron oxides onto the sand grain surface of porous media under mild chemical and temperature conditions. The technique involves sequential injections of a preconditioned ferrous iron solution and an oxidant solution and then orchestrate the advective-diffusive transport of the two reagents in porous media to create an overlapped reaction zone where ferrous iron is oxidized and precipitated on the sand grain surfaces. We demonstrate through bench-scale column tests the feasibility of using this technique to create a large-scale iron oxide-enriched reactive barrier in subsurface environment for *in situ* removal of arsenic. A sand filter with a fresh iron oxide coating can treat thousands of pore volumes of water contaminated with dozens of ppb arsenic before the coating needs to be regenerated. Arsenic breakthrough curves through the sand filter

suggest that both reversible adsorption and irreversible precipitation are responsible for removing arsenic from the water. Unlike conventional excavate-and-fill permeable reactive barriers, the treatment capacity of our *in situ* created barrier can be *in situ* regenerated and replenished with a fresh coating.

ACKNOWLEDGEMENTS

I would like to thank my committee chair, Dr. Huang, and my committee members, Dr. Karthikeyan and Dr. Deng, for their guidance and support throughout the course of this research.

Thanks also go to my friends and colleagues and the department faculty and staff for making my time at Texas A&M University a great experience.

Finally, thanks to my mother and father for their encouragement and to my wife for her patience and love.

NOMENCLATURE

PRB	permeable reactive barrier
MCL	maximum contaminant level
GFH	granular ferric hydroxide
IOCS	iron oxide-coated sand
EBCT	empty bed contact time
DO	dissolved oxygen
CDE	convection-dispersion equation
Eh	redox potential
K	reaction rate coefficient (dimensionless)
L	length (L)
ID	inside diameter (L)
C	resident concentration in the liquid phase (ML^{-3})
C_0	initial concentration in the liquid phase (ML^{-3})
z	vertical dimension of flow (L)
v_p	average pore velocity (LT^{-1})
D	longitudinal dispersion coefficient (L^2T^{-1})
μ	overall first-order decay coefficient (T^{-1})
R	retardation factor due to adsorption (dimensionless)
ρ_b	soil bulk density (ML^{-3})
θ	volumetric water content (dimensionless)

K_d	distribution coefficient of linear adsorption (L^3/M)
β	variable for partitioning in non-equilibrium transport models (dimensionless)
ω	mass transfer coefficient (dimensionless)

TABLE OF CONTENTS

Page

LIST OF FIGURES

Page

LIST OF TABLES

1. INTRODUCTION

1.1 Statement of problems

Arsenic has long been recognized as a toxicant since ancient times. Even at low concentrations, long-term exposure to inorganic arsenic can lead to a series of diseases, including skin tumors, liver dysfunction, gangrene, and hearing defect (Hutton, 1987). Effective on January 2006, the U.S. Environmental Protection Agency has lowered the maximum contaminant level (MCL) of arsenic in drinking water from 50 to 10 μg/L. The World Health Organization has the same 10 μg/L limit in its guideline for As.

Arsenic contamination of groundwater is a major health hazard for many regions of the world. It is estimated that 45 million to 57 million people in Bangladesh and 13 million in the United States are exposed to arsenic concentrations greater than 10 μg/L (WHO, 2006). In Texas, many groundwater sources in the Ogallala and Gulf coast aquifers often have arsenic concentrations above 50 μg/L (Fig. 1.1) (Regner et al., 2004).

Consequently, arsenic treatment of contaminated surface and groundwater is very important in order to supply people with safe drinking water. Various treatment processes, including oxidation, coagulation-precipitation, filtration and adsorption, have been used for arsenic removal for centralized public drinking water treatments. While the existing conventional treatment methods, although expensive, are adequate for such

---

This thesis follows the style of Water Research.

centralized treatments, there is a lack of a low cost, low maintenance, and high performance method suitable for removing arsenic for decentralized/household water supplies in many rural areas that are limited by the treatment cost and expertise.

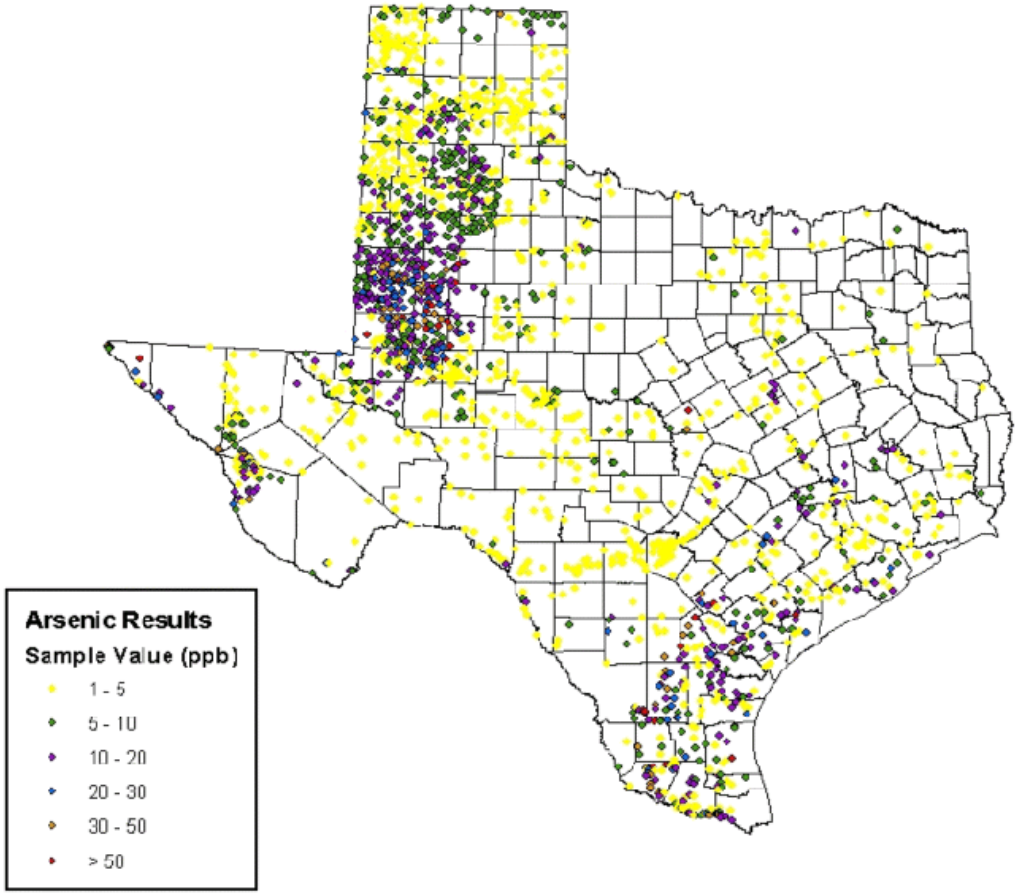

Fig. 1.1 - Groundwater arsenic contamination in Texas

For groundwater, using iron oxide-bearing minerals for treating arsenic-contaminated wastewater has long been of major interest because of iron oxides' extraordinary capability in adsorbing arsenic from water (e.g. Benjamin et al., 1993; Kundu and Gupta, 2007; Pokhrel and Viraraghavan, 2008). One application could be to

install an iron mineral reactive barrier surrounding a well for *in situ* arsenic removal. This application, however, has been limited due to the need of large scale and deep excavation of soils to emplace the reactive media (such as iron ore grains) and the difficulty to regenerate the adsorption capacity that could be consumed rapidly.

Although there are a few reported efforts to employ iron oxide-coated sands for various groundwater remediation including arsenic removal (e.g. Chang et al., 2008; Chen et al., 2007; Genz et al., 2008; Ko et al., 2007; Lenoble et al., 2005), none of existing coating procedures can be applied to *in situ* groundwater remediation without the need of a major excavation. As such, an *in situ* groundwater arsenic remediation using iron oxide-bearing minerals has not been a viable solution.

1.2 Research objectives

This study aims to develop a new environmental technique capable of *in situ* emplacing iron oxide coating on soil matrix to create a subsurface reactive barrier for remediation of arsenic-contaminated groundwater. The new technique avoids major excavation required by conventional permeable reactive barrier (PRB) techniques. Instead of preparing iron oxide-coated materials on the ground, our technique can directly coat subsurface soil matrix with iron oxides through injecting composited reactant solutions into porous media following a specially designed injection scheme. Laboratory-scale batch and column tests were conducted to demonstrate the feasibility of the concept we invented and evaluate the treatment capacity of the resulting iron oxide-coated sand bed.

2. TREATMENT OF ARSENIC WITH IRON OXIDES

2.1 Chemistry of arsenic

Arsenic chemistry in the aqueous phase is complicated due to the various oxidation states of atomic arsenic. Arsenic occurs in four oxidation states (-3, 0, +3 and +5). The predominant forms of arsenic in groundwater and surface water are the inorganic trivalent arsenite [As(III)] and pentavalent arsenate [As(V)] (Ferguson and Gavis, 1972).

As a water contaminant, As(III) is more problematic than As(V). Unlike the arsenate anions $H_2AsO_4^-$ and $HAsO_4^{2-}$, the dominant As(III) species up to pH 9.2 is the nonionic H_3AsO_3, which does not adsorb as strongly to mineral surfaces as As(V) (Hug and Leupin, 2003; Kanel et al., 2006). Table 2.1 shows approximate values for the pKa of inorganic arsenic species (Cherry et al., 1979). At normal natural pH environments (pH 4-9), $HAsO_4^{2-}$ and $H_2AsO_4^-$ are the dominant species for As(V) and H_3AsO_3 is for As(III).

Table 2.1 - The pK_a values of inorganic arsenic species

Arsenic species	pK_1	pK_2	pK_3
As(III): Arsenite	9.2	12.1	-
As(V): Arsenate	2.2	6.96	11.5

As(III) is thus more mobile in groundwater and is also more difficult to be removed in arsenic removal treatments. The distribution and mobility of dissolved arsenic species

are dependent on the pH and redox potential (Eh). The pH and Eh relationship is very important in understanding arsenic removal from water, arsenic immobilization/ stabilization on solid phases as well as the distribution of arsenic species in water. Fig. 2.1 illustrates the effect of pH and Eh (or pE) on major arsenic species at equilibrium conditions (Welch et al., 1988).

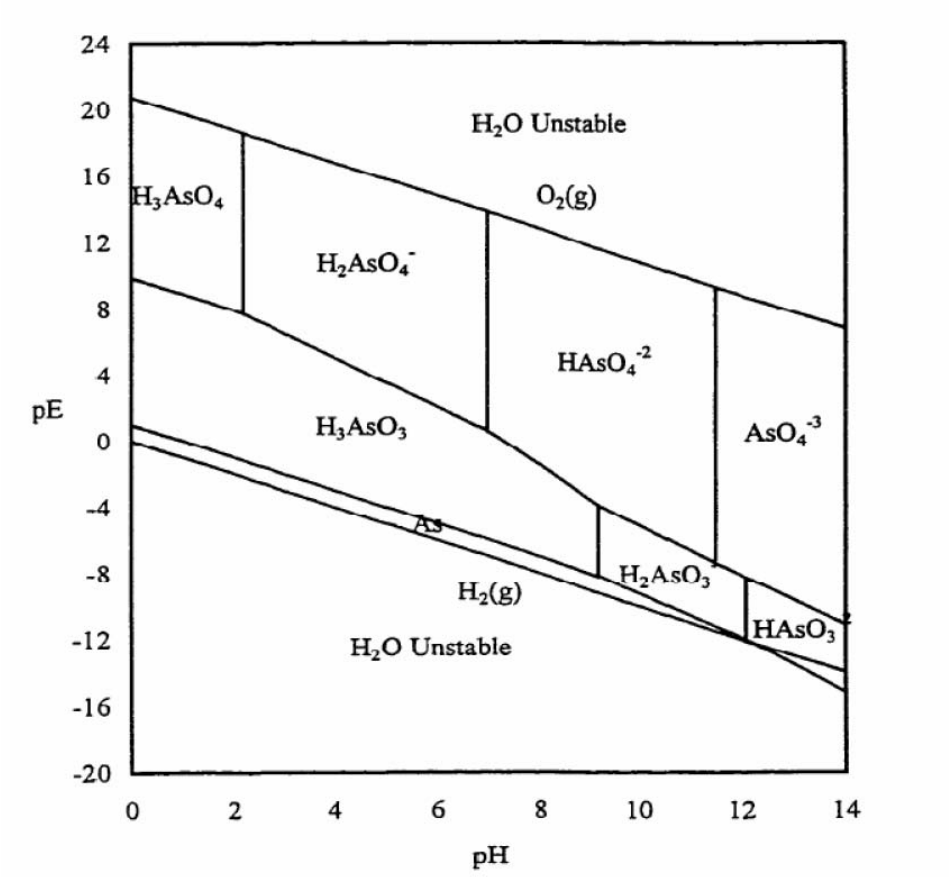

Fig. 2.1 - pE/pH diagram for the As-H_2O system at 25℃

Typically, oxidation of As(III) As(V) is a necessary step in many arsenic removal processes. Although As(V) is thermodynamically favored under aerobic conditions, As(III) is only slowly oxidized by dissolved O_2, with a half-life of around 9d in air-saturated water with low iron contents and pH 7.6-8.5 (Kim and Nriagu, 2000). The As(III) oxidation by H_2O_2 is also slow at neutral and acidic pH, as only $H_2AsO_3^-$ and $HAsO_3^{2-}$ but not H_3AsO_3 react with H_2O_2. The half-life of As(III) in 1 mM H_2O_2 at pH 7.5 is 2.1 d.

2.2 Arsenic removal by iron (hydr)oxide

Arsenic adsorption on iron (hydr)oxide surfaces has received significant attention and much research is underway because of its effective removal of arsenic and ease of operation and handling. Iron hydroxides such as goethite and ferrihydrite, commonly found in soils, influence the mobility behavior of As (Aguilar et al., 2007). The most common iron hydroxides are ferrihydrite (β-FeOOH), lepidocrocite (γ-FeOOH), goethite (α-FeOOH), and hematite (α-Fe_2O_3). Goethite and hematite are the most stable ones.

Iron hydroxides are promising sorbent materials for arsenic because they have strong chemical affinities and large specific surface areas. Adsorption of As by iron(II)/(III) hydroxide (green rust) and iron(III) hydroxides such as goethite and lepidocrocite has been proved to be two or more orders of magnitude greater than arsenic adsorption by silicate clays and feldspars (Lin and Puls, 2003).

Two principal processes are responsible for As geochemistry in groundwater in the presence of iron compounds: adsorption of As(V) and As(III) on iron hydroxides and

precipitation of secondary phases such as iron arsenates (Pedersen et al., 2006). Under oxidizing conditions, As(V) is retained in the solid phases by interaction with Fe(III) oxy-hydroxide coatings on soil particles (Bose and Sharma, 2002). The mechanism involved in the adsorption of As species into iron oxides, including poorly crystalline oxides such as ferrihydrite, is the replacement of OH_2 and OH^- for the anionic As species in the coordinate spheres of surface structural Fe atoms, resulting in monodentate, bidentate, mononuclear, or binuclear bridging complexes (Jain et al., 1999; Raven et al., 1998; Miretzky and Cirelli, 2010).

Although iron hydroxides exist naturally in divalent and trivalent oxidation state, they can be synthesized. Iron hydroxides formed under different conditions have different adsorption efficiency, color, surface properties, and mineralogical characters. Their formation depends on temperature, pH, aging time, electrolyte composition, and oxygen in water. The preferable temperature and pH for their formation are 60-70°C and 6-10, respectively (Benjamin et al., 1993). The amount of hydroxyl groups available on the iron hydroxide surface is used as a criterion to measure the surface site density. The reported site densities for hematite, goethite, and ferrihydrite in the literature are 0.02, 0.05-0.1, and 0.87-0.91 mol site / mol Fe, respectively (Balistrieri and Murry, 1983; His and Langmuir, 1985).

Dozens of iron (hydr)oxide-based sorbents have been investigated, such as: granular ferric hydroxide (GFH) (Badruzzaman et al., 2004; Sperlich et al., 2005), activated carbon-based iron oxide-containing sorbents (Gu et al., 2005; Vaughan and Reed, 2005), nanostructured hydrous iron oxide-coated polymeric beads (Sylvester et al., 2007), and

iron oxide-coated sand (Benjamin et al., 1996). The iron oxide-coated sand filter system, as an emerging technology, affords several advantages, including: (1) highly sorptive properties against the contaminants; (2) formation of highly porous media with minimal clogging risks; and (3) easy possible regeneration and reuse to amend the reactive properties (Ko et al., 2007).

Table 2.2 presents a summary of arsenic adsorptive capacities, calculated at 20 μg/L aqueous arsenic concentration, and cost effectiveness of the iron oxide-coated sand. The estimated arsenic removal cost of the iron oxide-coated sand is $3.3-4.2/ g As, supporting the current trend towards the use of metal hydroxide media.

Table 2.2 - Adsorption capacities of iron oxide-coated sands for arsenic

Reference	pH	Sorption Density (mg As/g)	Bed Volumes Treated	Material Cost ($/ton)	Cost of Arsenic removal ($/g As)
Joshi and Chaudhuri (1996)	7.5-7.8	0.1	150	100	1.00
Vaishya and Gupta (2003)	7.2-7.4	0.09	125	100	1.18
Vaishya and Gupta (2003)	7.2-7.4	0.04	54	100	2.70
Thirunavukkarasu et al. (2003a)	7.6	0.03	1,000	100	3.33
Benjamin et al. (1996)	8.0	0.02	600	100	5.00

2.3 Iron oxide coatings

These iron oxide coatings have been developed by using two methods: adsorption and precipitation (Xu and Axe, 2005). In the adsorption method, iron solution is first prepared using an iron source such as ferric chloride or ferric nitrate, the solution pH is adjusted to the required coating pH with acid or base, and then the substrate is submerged in the iron solution/precipitate for the desired duration at the desired temperature (room or higher temperature) (Xu and Axe, 2005; Benjamin et al., 1996). In the precipitation method, the pH of the iron solution is adjusted in the presence of substrate and then the substrate is maintained in the iron solution/precipitate for the desired duration at the desired temperature (room or higher temperature). Solution pH determines the iron species present in solution during coating process. The relevant chemical reactions are shown below (Westall et al., 1976):

$FeOH^{2+} + H^{+} \leftrightarrow H_2O + Fe^{3+}$ Log K = -2.187

$Fe(OH)_2^{+} + 2H^{+} \leftrightarrow 2H_2O + Fe^{3+}$ Log K = -4.594

$Fe(OH)_3 + 3H^{+} \leftrightarrow 3H_2O + Fe^{3+}$ Log K = -12.56

$Fe(OH)_4^{-} + 4H^{+} \leftrightarrow 4H_2O + Fe^{3+}$ Log K = -21.588

At acidic coating pH conditions, iron binds with substrates through an ion exchange process (i.e., replaces H^{+} ions from substrates) and at basic coating pH conditions, iron hydroxide precipitates deposit on substrates (Benjamin et al., 1996; Zeng, 2003; Xu and Axe, 2005). Coating temperature determines the strength and iron oxide phase of the

oxide coating (Benjamin et al., 1996). High temperature treatment provides a stronger iron oxide coating, but at the expense of its arsenic adsorptive capacity as more crystalline iron oxide phases have lower adsorptive capacities than amorphous or lesser crystalline iron oxide phases (Benjamin et al., 1996; Schwertmann and Cornell, 2000).

For iron oxide-coated adsorbents, the extent of iron loading depends on substrate properties (i.e., specific surface area and availability of surface functional groups capable of binding iron oxide, such as silanol, hydroxyl, carboxyl, ammonium, etc.), and coating conditions (i.e., coating temperature, pH, initial iron concentration, and duration used). Previous studies have used different combinations of coating temperature (ranging from 25°C to 110°C), coating pH (ranging from acidic to basic pH) and initial iron concentration (ranging from 0.001 M to 2.5 M) to produce iron loadings of 0.025 to 468 mg Fe/g media on different substrates.

3. MATERIALS AND METHODS

In this study, we employed *in situ* reactions to produce an iron oxide coating on sand media. Column flow-through tests were performed to further elucidate the mechanism of iron oxide generation.

3.1 Materials

All chemicals used in this study were of analytical grade and were purchased from VWR or Fisher Scientific. E-pure de-ionized water (Barnstead) was used to prepare reagent solutions throughout this study. Prior to use, all glassware and polyethylene bottles were cleaned by soaking in 5% hydrochloric acid for at least 24 hours and then rinsing with de-ionized water three times. For iron oxide coating experiments used three feeding solutions: a ferrous ion solution prepared with $FeCl_2$; an oxidant solution prepared with NaClO, and a tank of DI water. All three solutions were prepared with de-oxygenated water and remained anaerobic during the coating experiment. The pH of the three solutions was adjusted with HCl or NaOH to the desired value. Deoxygenated DI water was prepared by flushing water with nitrogen gas (industrial grade) in a capped container for at least one hour and then stored in an anaerobic chamber overnight before use. During the experiments, the three feeding bottles were sealed with a cap with headspace continuously flushed with nitrogen gas to prevent dissolved oxygen from entering the test solutions and the sand column. Prior to use, silica sand (collected between US sieves#40 and #60, with grain diameter measured between 0.25 and 0.43

mm) was washed twice in 6 N HCl solution to remove impurity such as surface-attached clay particles and iron oxides, and was then rinsed and preserved in de-ionized water before use.

3.2 Analysis methods

Arsenite was analyzed by an ion chromatography system (Dionex DX500) equipped with absorbance detector AD20. The method used AS18 (Dionex) separation column; the eluent was 16mM NaOH with a flow rate of 1.2 mL/min. Wave length of the absorbance detector was set at 215nm with UV low. Under the selected conditions, arsenite ion had a retention time of 2.75 min.

Arsenate and chloride were analyzed by Dionex DX500 equipped with conductivity detector CD20. The method also used AS 18 Separation column; the eluent was 30mM NaOH with a flow rate of 1.2 mL/min; the SRS current was 100mA. Under the selected conditions, retention time of chloride and arsenate was 3.69 and 11.06 min, respectively.

Ferrous ion was analyzed by phenanthroline method according to the US EPA Method 3050B: (1) Acidify each sample with 0.1 mL 3N HCl / 5 mL sample at time of collection. (2) Withdraw 2-mL portion of acidified sample and add 4 mL ammonium acetate buffer solution (dissolve 40 g $NH_4C_2H_3O_2$ and 50 mL glacial acetic acid to 1L solution) and 1 mL phenanthroline solution (dissolve 1 g 1,10-phenanthroline monohydrate, $C_{12}H_8N_2 \cdot H_2O$, in 1 L water). (3) Dilute to 10 mL with vigorous stirring. (4) Measure color intensity within 10 min at 510 nm wavelength, using T80+ UV-VIS

spectrometer. (5) The absorbance of sample is corrected by reference to the control containing the same amount of buffer and phenanthroline.

All experiments and measurement were conducted in duplicate.

3.3 Iron oxide coating procedure

3.3.1 Column packing

A glass chromatography column (Kontes Chromaflex) that measures 30 cm in length and 4.8 cm in inside diameter with nominal volume of 543 mL was packed with pre-cleaned silica sand for iron oxide coating experiments (Fig. 3.1). The column dimensions met the minimum requirement of $L \geq 4 \times ID$ to ensure that the effective porosity is constant. Wet packing method was used. To pack a more uniform sand column, the clean sand was added to de-ionized water in the column with vigorous stirring (with a stick) to release any bubble trapped in the sand. The column was sealed by two caps with a flow adapter on it (Fig. 3.1).

The porosity of saturated sand is determined to be 37.9% by comparing the weight of dry sand of 100 mL with that of the same amount of sand but saturated in water. Thus the volume of water in a saturated column is 543 mL × 37.9% = 206 mL. The weight of dry sand in the column, measured by a balance, is 916 g ± 5 g.

Fig. 3.1 – Glass chromatography column packed with clean silica sand

3.2.2 Four-steps injection cycle

Emplacement of iron oxide on sand media was achieved through a cyclical four-step procedure. As illustrated in Fig. 3.2, each injection cycle consists of four steps, alternatively injecting $FeCl_2$ solution, NaClO solution, and water. The idea behind this innovative *in situ* coating technique is to deliver ferrous ion (Fe^{2+}) and oxidant (e.g., H_2O_2 and ClO^-) separately into the deep soil media so that the clogging due to the rapid precipitation of iron oxide formed upon direct contact between Fe^{2+} and the oxidant can be avoided. To prevent the immediate direct contact between Fe^{2+} and the oxidant,

deoxygenated water was injected in-between to provide a buffer zone that separates Fe^{2+} plume and oxidant plume. The parameters that will affect where and how rapidly iron oxide coating could be formed include Fe^{2+} concentration, oxidant concentration, type of oxidants, flow rate, and the duration of each injection.

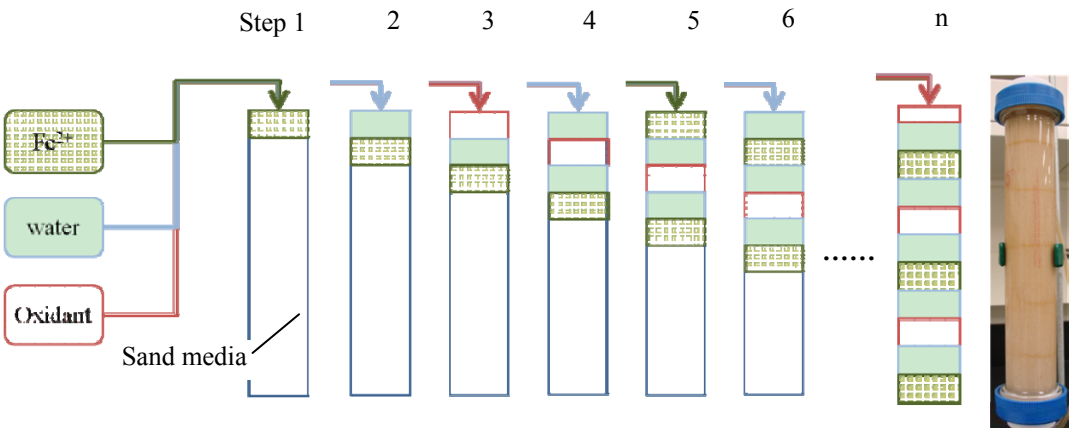

Fig. 3.2 - Operation scheme for *in situ* emplacing iron oxide coating on porous media.

In a typical coating experiment, the following procedure was employed for each 4-min coating cycle composed of four 1-min steps:

Step 1: Starting at t=0 min, 2 mM ferrous chloride ($FeCl_2$) solution was injected to the top of the sand column at the flow rate of 12.1 mL/min. The flow rate resulted in an empty bed contact time (EBCT) of 17 min. The $FeCl_2$ solution was prepared and maintained under anaerobic condition (DO < 0.1 mg/L).

Step 2: Starting at t=1 min, deoxygenated DI water was injected into the column at the same flow rate of 12.1 mL/min.

Step 3: Starting at t=2 min, 1 mM sodium hypochlorite (NaClO) was injected at the same flow rate of 12.1 mL/min.

Step 4: Starting at t=3 min, deoxygenated DI water was injected at the same flow rate. After Step 4, the system returns to Step 1 and starts a new coating cycle. Steps 2 and 4 provide a water buffer to separate direct contact between Fe^{2+} and oxidant. In this exemplary procedure, the injection lasts for one minute for each of the four steps. In real application, the duration of each injection could be adjusted depending on the actual coating results. For example, increasing the injection duration of water (Steps 2 and 4) increases the separation of Fe^{2+} and ClO^-, thus delays the timing when Fe^{2+} comes into contact with ClO^-. As a result, oxidation and precipitation of Fe^{2+} occurs at a farther distance from the injection point.

The column was operated continuously following this four-step cycle until a heavy brownish color of iron oxide was developed on sand grain surface. A programmable 3-way valve was employed to switch the inflow automatically before the peristaltic pump. The mass of NaClO provided in each cycle could stoichiometrically oxidize and precipitate Fe^{2+} injected.

3.3.3 Iron content in the column

Iron content of the coated sand was determined using acid digestion technique. 10 g of the coated sand (dry mass) was added to approximate 100 mL 6N HCl solution in a beaker. The mixture was shaken for 30 minutes and left overnight. After 12 hours, the HCl wash solution was collected; the sand was washed with 6N HCl solution again

until the sand appeared clear with no visible brownish color or stain, which indicates a complete dissolution of iron oxide coating of the sand. The extracting HCl solution was made up to 1.00 liter with de-ionized water, and analyzed for dissolved iron concentration using ion chromatography.

3.4 Column flow-through experiments

Column flow-through experiments were conducted to determine adsorption and precipitation characteristics of reactants (e.g., Fe^{2+}) and pollutants (e.g. arsenite and arsenate ions) when passes through sand-packed columns under different conditions. In general, the breakthrough curves from these tests were used to explain how and under what conditions iron oxides could be more effectively formed *in situ* and what amount of arsenic the iron oxide-coated sand bed could remove before its adsorption capacity is exhausted. The experimental set-up is shown in Fig. 3.3.

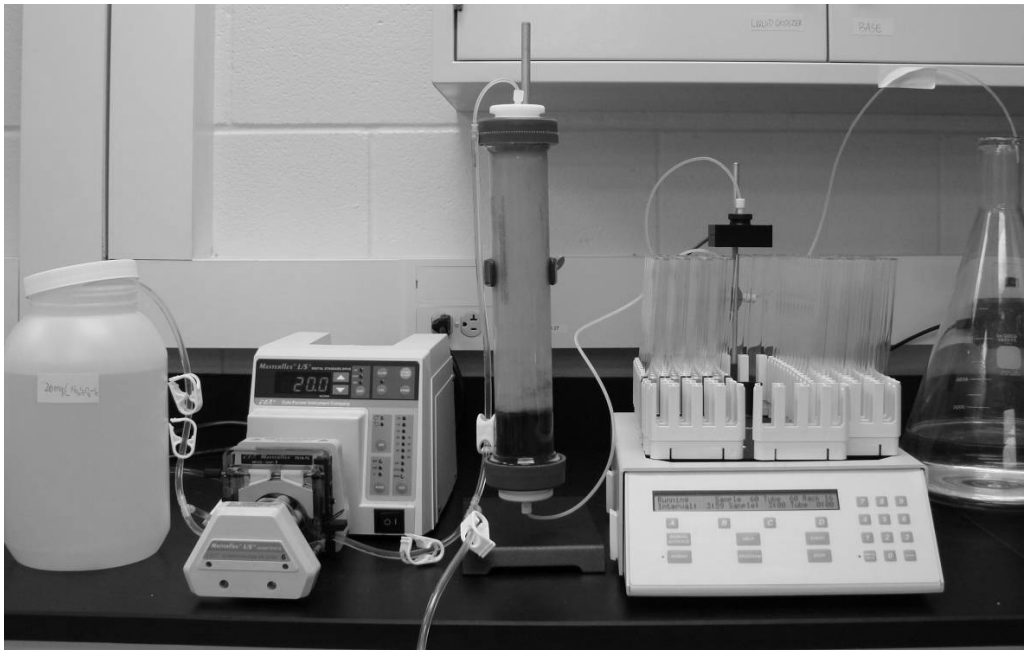

Fig. 3.3 - Experimental set up for column flow-through tests. From left to right: influent container, MasterFlex peristaltic pump, glass column, interval sampler, effluent container.

3.4.1 Sodium chloride tracer test

Chloride (from NaCl) was used as a conservative tracer to determine the dispersion coefficient of dissolved chemicals in the saturated sand media of the column under typical coating conditions. Before conducting a tracer test, the column was flushed with DI water for at least 10 pore volumes. 10 mM NaCl solution was then injected into the sand column as a step function with the flow rate controlled at 12.1 mL/min. In total, six pore volumes of NaCl were injected. Effluent samples were collected from the bottom of the column using a fraction collector with a sampling interval of 30 seconds. The

samples were analyzed with ion chromatography for chloride concentrations. The results were used to construct a Cl^- breakthrough curve.

3.4.2 Ferrous chloride breakthrough tests

Column breakthrough tests were conducted to study the Fe^{2+} adsorption/precipitation characteristic on clean sand and iron oxide-coated sand surface under simulated groundwater chemical environments. Simulated groundwater was prepared in the laboratory as Table 3.1. $CaCl_2.2H_2O$, $MgSO_4.7H_2O$, $NaHCO_3$, KCl, NaF, and H_2SO_4 were used to prepare the simulated groundwater. The pH was adjusted using HCl or NaOH to either 6.0 or 7.0.

Table 3.1 – Simulated groundwater characteristics

Parameter	Simulated groundwater
Ca^{2+} (mg/L)	60
Mg^{2+} (mg/L)	15
Na^+ (mg/L)	59
K^+ (mg/L)	3
HCO_3^- (mg/L)	150
SO_4^{2-} (mg/L)	76
Cl^- (mg/L)	109
F^- (mg/L)	2
Alkalinity (mg/L)	105
pH	7.3

Before test, the column was flushed with simulated groundwater for at least 10 EBCTs to equilibrate the column. At time zero, 20 mg/L $FeCl_2$ (as Fe) spiked in the simulated groundwater was injected to the sand column as a step function. The flow rate was controlled at 7.2 mL/min, corresponding to an EBCT of 28.6 min. After 172 min (6 EBCTs), the $FeCl_2$ solution was replaced by simulated groundwater without iron. Effluent was collected by a fraction collector at a sampling interval of 30 seconds. The samples were analyzed for pH and Fe^{2+} concentration. The breakthrough curves of Fe^{2+} was constructed and analyzed to understand the adsorption, precipitation, and desorption behavior of Fe^{2+} in both clean silica sand bed and iron oxide-coated sand bed.

3.4.3 Arsenite and arsenate breakthrough tests

Arsenite and arsenate breakthrough tests were conducted to investigate the adsorption characteristics of As on iron oxide-coated surface and its dependence on pH. Similar to Fe^{2+} breakthrough tests, the simulated groundwater spiked with 20 mg/L $NaAsO_2$ (as As) and 20 mg/L Na_2HAsO_4 (as As) was injected into the sand column as a step function at a flow rate of 7.2 mL/min (corresponding to an EBCT of 28.6 min). After 172 min (6 EBCT), the $NaAsO_2$ and Na_2HAsO_4 solution was replaced by simulated groundwater without arsenic to study adsorption/desorption/precipitation of arsenic in the column. Samples were collected for every 30 seconds and analyzed for pH, arsenite and arsenate concentration.

4. RESULTS AND DISCUSSION

4.1 *In situ* iron oxide emplacement

The pictures in Fig. 4.1 show that the development of an iron oxide coating on sand bed over a time span of 96 h. The initial sand surface had a white color that is typical of clean silica sand surface. The coating solutions and delivery sequence were: 1 min 2 mM $FeCl_2$ → 1 min DI → 1 min 1 mM NaClO → 1 min DI; flow rate Q = 12.1 mL/min; the pH of three coating solutions were pre-adjusted to 7.0 using 50 mM of HEPES buffer. Once coating procedure was started, the sand in the column rapidly developed a brownish iron oxide coating within a few hours. The coating was rather uniform along the sand bed. The sand bed was well coated with iron oxide in 4 days. The well-coated sand has iron content in the range of 1.6 to 2.0 mg Fe/ g sand.

The idea behind this innovative *in situ* coating technique is to deliver ferrous ion (Fe^{2+}) and selected oxidant (like ClO^-) separately into the deep soil media. To prevent the direct contact between Fe^{2+} and oxidant that could lead to rapid precipitation of iron oxides concentrated in the inlet zone and cause clogging problem, we used a water plug to separate Fe^{2+} plume and oxidant plume. This solution is simple but very effective. The underlying mechanism is not straightforward. The development of the technique requires in-depth understanding of iron chemistry and the advective-diffusive-reactive transport processes in porous media. Fe^{2+} can be oxidized in a controllable manner when flowing through the column by controlling the timing and extent of contact between Fe^{2+} and oxidant through injection and hydraulic control. The pH is another important

parameter because both adsorption of Fe^{2+} on sand surface and oxidation of Fe^{2+} depend significantly on pH.

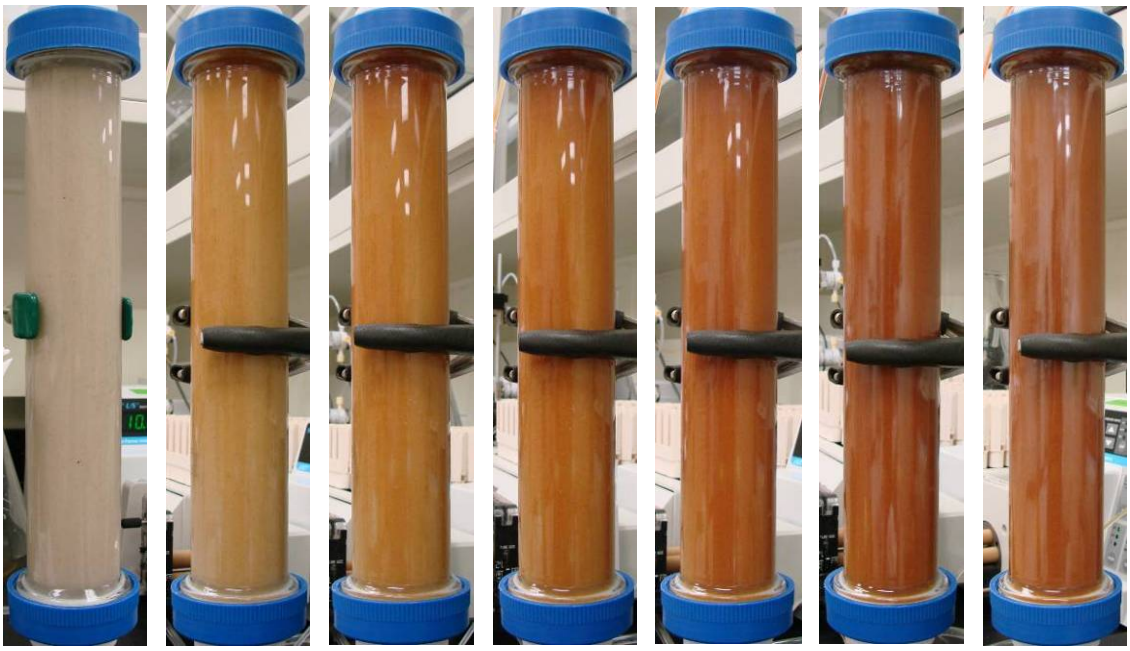

Fig. 4.1 - Emplacement of iron oxide coating on sand grains through periodically injections of ferrous iron solution and hypochlorite (oxidant) solution that is buffered with a water plug.

Several trial tests were conducted before achieving this success. It was found that concentration of reagent solutions, pH of solutions, dissolved oxygen control, and injection durations affected the coating process. In the absence of injecting a water buffer between Fe^{2+} and ClO^-, oxidation and precipitation of Fe^{2+} concentrated in the inlet zone (the first two inches). As a result, the inlet zone was rapidly clogged due to excessive accumulation of iron oxide precipitate. The coating process could not be continued even though the main section of column below the inlet zone still remained

largely clean with adequate hydraulic conductivity. The second approach to avoid the local excessive accumulation of iron oxide precipitates was to control the pH of reactant solution. As has been well understood and documented, the oxidation and precipitation of Fe^{2+} depends significantly on the pH. When the pH of Fe^{2+} and ClO^- solutions was appropriately controlled to be slightly acidic, for example, the reaction rate of Fe^{2+} oxidation and precipitation was greatly reduced and thus clogging of iron oxides in the inlet zone could be avoided. In a trial test, we were able to form iron oxide coating first near the bottom (outlet) of sand column before the coating progressed towards the inlet zone on the top.

Fig. 4.2 illustrates the oxidation of Fe^{2+} due to diffusion. Five brown bands appeared on the sand bed after the continuous coating process was interrupted and stopped in a trial test. While the feeding of reagents was stopped, both Fe^{2+} and ClO^- bands in the column continued to diffuse toward each other. When the two reactants met in the middle of the water band that initially separated Fe^{2+} and ClO^-, Fe^{2+} was oxidized and precipitated to form a brownish ring. The location of these bands matched the injection intervals perfectly (see Fig. 3.2): there were five water zones, three iron zones and three oxidant zones alternately in the column. Fe^{2+} reacted with ClO^- in the water zones after the two diffused and came to contact and react to form brownish iron oxide precipitation. There was no such visible brown band during continuous coating experiments. Under normal coating procedures, the reactive zone would not stagnate at a specific site to form a visible ring but migrate together with the bulk flow of the two reactant plumes and coated the sand bed more uniformly.

The successful *in situ* emplacement of iron oxides on the sand-packed column has proven the feasibility of the concept we invented. The sequential injection technique in conjunction with pH control has the potential to solve the problem of clogging in the inlet (or injection) zone. In particular, the insertion of a water buffer to separate the two reactants and delay their contact is a creative yet simple solution that can control how far from the injection point the iron oxide precipitation reaction could start to occur in the porous media. The successful emplacement clearly demonstrates the potential of using the technique to create a large-scale subsurface iron oxide-based reactive barrier for groundwater remediation.

Fig. 4.2 – Reaction zones illustrated by five brown bands formed under stagnant conditions.

4.2 Breakthrough curves of Fe^{2+}

Column breakthrough tests using Fe^{2+} as a tracer were conducted with simulated groundwater to investigate how Fe^{2+} transport through the sand-packed column under various conditions. One objective is to understand the different adsorption behavior of Fe^{2+} on clean sand versus iron oxide-coated sand. In addition, the tests will help evaluate how pH will affect the adsorption behavior and whether the adsorption of Fe^{2+} on sand surface is reversible or irreversible. Improved knowledge of how Fe^{2+} transport through the porous media under various conditions could deepen our mechanistic understanding of how iron oxide is emplaced on the sand surface and provide guidance to optimize the coating technique to avoid the clogging problem and other potential problems.

The Fe^{2+} breakthrough test was conducted under the following conditions: 20 mg/L $FeCl_2$ (as Fe) spiked in the simulated groundwater was injected to the sand column as a step function with the flow rate of 7.2 mL/min, corresponding to EBCT of 28.6 min. After 172 min (6 EBCT), the $FeCl_2$ solution was replaced by simulated groundwater without iron.

4.2.1 Effect of pH and iron oxide coating on Fe^{2+} adsorption

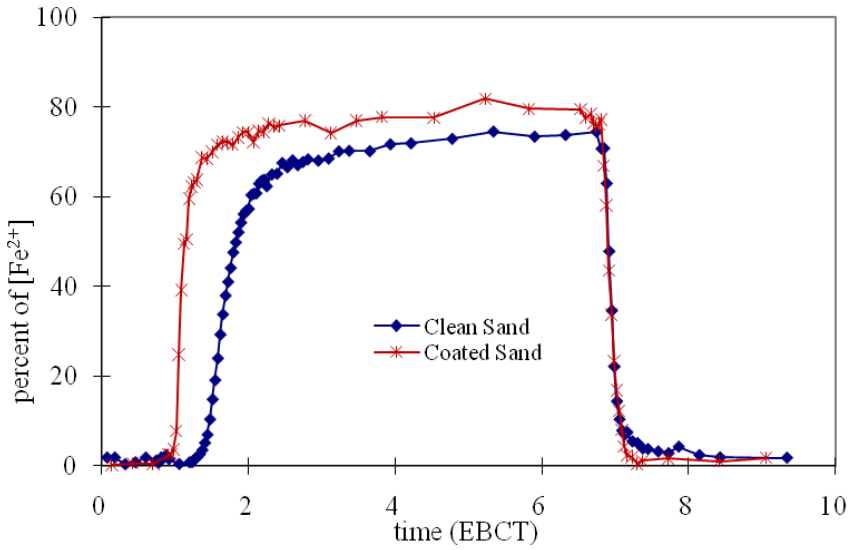

Fig. 4.3 – Fe^{2+} breakthrough curves on clean sand and iron oxide-coated sand at pH 6.0.

Fig. 4.3 shows Fe^{2+} breakthrough curves on clean sand and iron oxide-coated sand at pH 6.0. For iron oxide-coated sand, Fe^{2+} breakthrough occurs almost immediately after the first EBCT, which means that adsorption of Fe^{2+} on iron oxide surface was insignificant. The concentration of Fe^{2+} after breakthrough, however, was only 70-80% of that in the feed solution, which means that a portion of Fe^{2+} could be lost through precipitation. For clean sand, Fe^{2+} breakthrough occurred at t = 1.5 EBCT, which means that there was a noticeable adsorption of Fe^{2+} on silica sand surface at pH 6.0. Similarly, the concentration plateau of Fe^{2+} could only reach to about 70% of the feed, suggesting that precipitation of Fe^{2+} occurred. While Fe^{2+} feeding was stopped at t = 6 EBCT, the dropping limp of Fe^{2+} breakthrough emerged almost exactly after one EBCT at t = 7

EBCT and rapidly reached to an insignificant level. The lack of significant tailing suggests that desorption was not playing a significant role in both clean sand and iron oxide-coated sand. Lack of desorption suggested that the adsorption was irreversible; i.e., the adsorbed Fe^{2+} would eventually be precipitated.

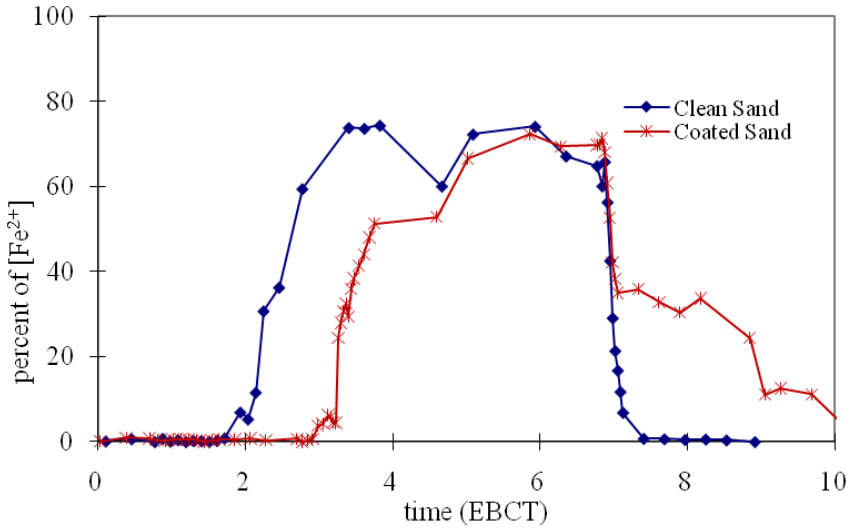

Fig. 4.4 – Fe^{2+} breakthrough curves on clean sand and iron oxide-coated sand at pH 7.0.

Fig. 4.4 shows Fe^{2+} breakthrough curves obtained on clean sand and iron oxide-coated sand at pH 7.0. The clean sand produced similar Fe^{2+} breakthrough curves at pH 6.0 and 7.0 (Fig. 4.5). The major difference is that the rising limp appeared at about 2.0 EBCT at pH 7.0, compared to at about 1.5 EBCT for pH 6.0. This means that the clean sand surface has a stronger adsorption at pH 7.0 than at pH 6.0. The change of pH could affect the adsorption behavior through two mechanisms. First, increase of pH from 6.0 to 7.0 will likely increase the negative charge of silica sand surface and therefore increase adsorption of positive charge of Fe^{2+} (or $FeOH^{+}$). Quartz (SiO_2) has an isoelectric point

near pH 3. At pH > 3, sand surface will carry more negative charge as pH increases. For iron oxide-coated sand, a change of pH from 6.0 to 7.0 appears to have significantly increased the adsorption behavior of Fe^{2+} on iron oxide surface (Fig. 4.6). The large tail of the dropping limp suggests that the adsorption of Fe^{2+} was partially reversible. This could be due to two mechanisms. Most of iron oxides are neutral or carry a weak positive charge at near neutral pH. For example, lepidocrocite and hematite have point of zero charge at pH 7.4 and 8.4, respectively. As such, the iron oxide coating surface could carry more positive charge at pH 6.0 than pH 7.0. Therefore, adsorption of Fe^{2+} will be more difficult at pH 6.0. From another perspective, when contact water, iron (hydr)oxide surfaces become hydroxylated due to adsorption of a monolayer of water molecules; each hydroxylated site could release one or two protons and transform to $–FeOH_2^+$, $–FeOH^0$, or $–FeO^-$. pH will dictate which form will dominate. Adsorption of Fe^{2+} onto iron hydroxide surfaces occurs when ions of opposite charge accumulate onto the oxide surface and the entire aqueous solution declines to electroneutrality. Thus the iron hydroxide adsorbs more ferrous ion at higher pH. From the breakthrough pattern, it appears that at pH 6.0, there is no significant Fe^{2+} adsorption on the coating surface; precipitation, however, could be significant and account for about 20% of loss during the flow through. At pH 7.0, there is significant reversible adsorption. Precipitation also increases at pH 7.0. It is interesting to note that some of the adsorbed Fe^{2+} could be released. Outer-sphere adsorption could be reversed.

Results of Fe^{2+} breakthrough tests suggest that increasing pH will increase adsorption of Fe^{2+} and thereby expedite the formation of an iron oxide coating when

those adsorbed Fe^{2+} is exposed to strong oxidant during the subsequent oxidant injection phase.

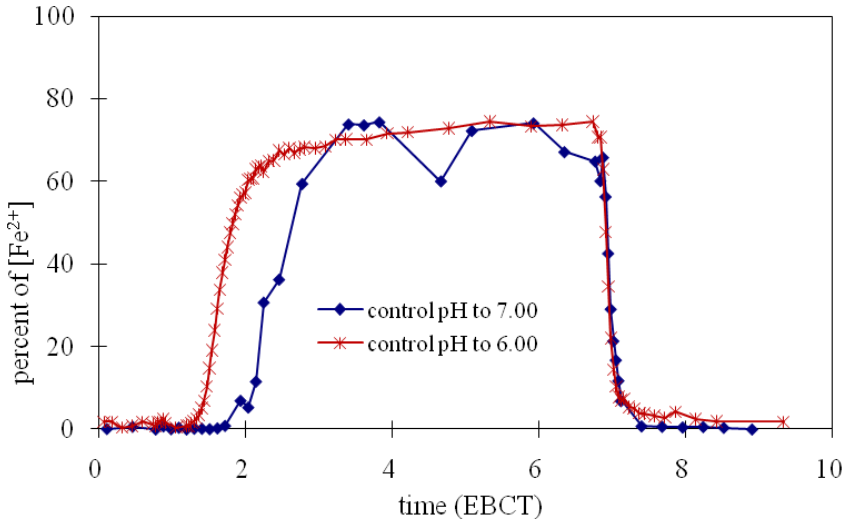

Fig. 4.5 – Fe^{2+} breakthrough curves on clean sand at pH 6.0 and 7.0.

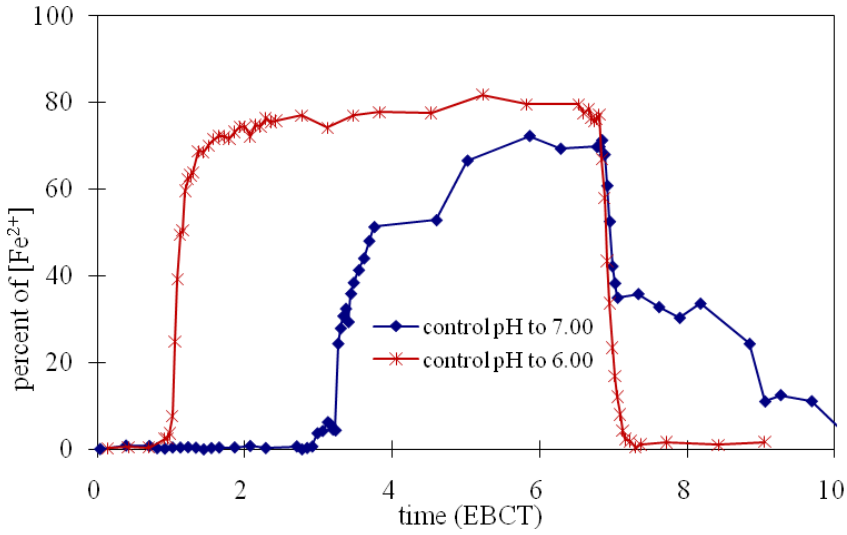

Fig. 4.6 – Fe^{2+} breakthrough curves on iron oxide-coated sand at pH 6.0 and 7.0.

4.2.2 Effect of previous breakthrough test on new test

Right after running the breakthrough curve test at pH 7.0, a second Fe^{2+} breakthrough test was performed under the same conditions (Fig. 4.7). Compared with Fig. 4.4, both clean sand and iron oxide-coated sand has similar breakthrough time. The second test, however, the curves, especially for clean sand, reached a higher Fe^{2+} concentration during the plateau stage, which means that less Fe^{2+} was precipitated during the second breakthrough tests.

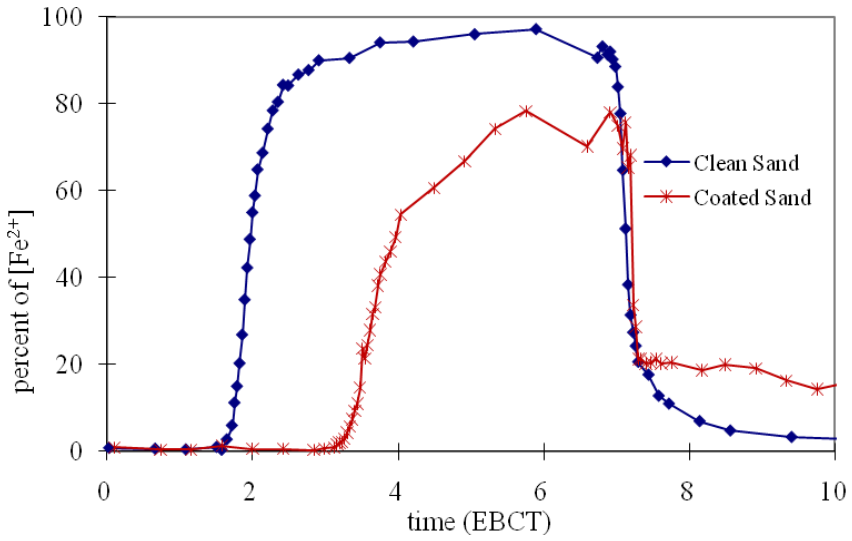

Fig. 4.7 – Fe^{2+} breakthrough curves on clean sand and iron oxide-coated sand at pH 7.0.

4.2.3 Mechanism of in situ iron oxide coating

From the above breakthrough results, two mechanisms are proposed here as a viable mechanism for *in situ* generation of iron oxide in a sand bed.

First, Fe^{2+} could be oxidized and then precipitated from aqueous phase to form FeOx particles. The particle could then deposit on sand grain surfaces. Contact of Fe^{2+} (or other aqueous ferrous species such as $FeOH^{+}$ or $Fe(OH)_2$) with oxidant is required for a homogeneous reaction to occur. Such contact could happen when the two reagent plumes diffuse toward each other during their advective transport through the sand bed. Such homogeneous contact will be enhanced if the transport of Fe^{2+} through the sand media is retarded due to significant adsorption/desorption and the plume was caught up by the subsequent oxidant plume that travel without retard.

Second, Fe^{2+} could be adsorbed and precipitated on the sand grain surface to form surface-bound Fe(II). Such s.b.Fe(II) could then be oxidized through heterogeneous reaction when oxidant plume pass.

Heterogeneous precipitation and formation of iron oxide coating is preferred for several reasons. First, it may produce more uniform coating throughout the column. Second, heterogeneous process could form a coating that is chemically bound to the sand grain surface and therefore is more stable and less likely remobilized. Third, heterogeneous precipitation is less likely to clog the sand bed. In the homogeneous process, deposition of FeOx particle may concentrate on certain limited area or pore structures and therefore is more prone to clog the sand bed.

4.3 Breakthrough curves of arsenic

Arsenic breakthrough tests were to evaluate the effectiveness of iron oxide coating in filtering out dissolved arsenic. It must be noted that the test concentration for As is 20

mg/L. For most of As-contaminated groundwater used as drinking water source, a typical concentration is in tens of ppb level.

4.3.1 Effect of pH and iron oxide coating on arsenic adsorption

Figure 4.8 and 4.9 shows that both arsenate and arsenite can penetrate the clean sand bed with almost zero retardation and removal for both pH 6.0 and 7.0.

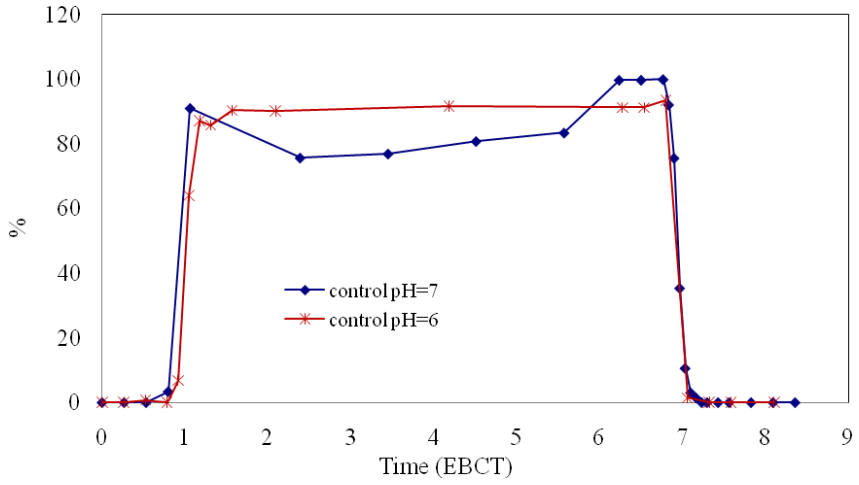

Fig. 4.8 – As(V) breakthrough curves on clean sand at pH 6.0 and 7.0.

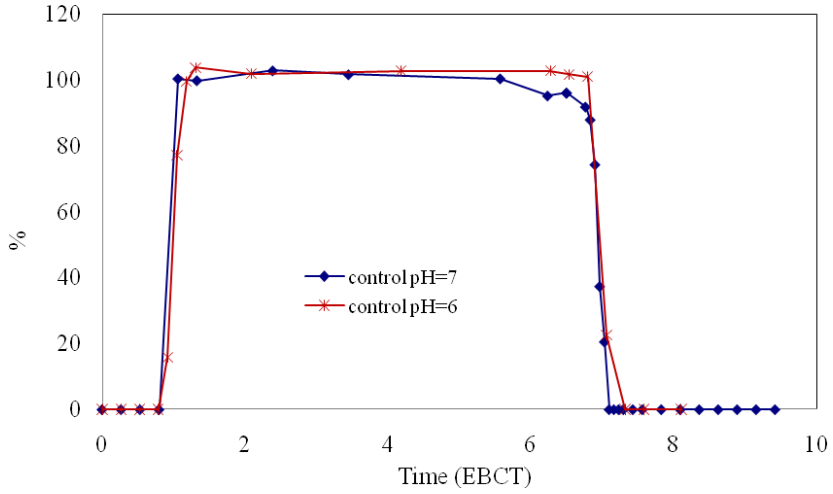

Fig. 4.9 – As(III) breakthrough curves on clean sand at pH 6.0 and 7.0.

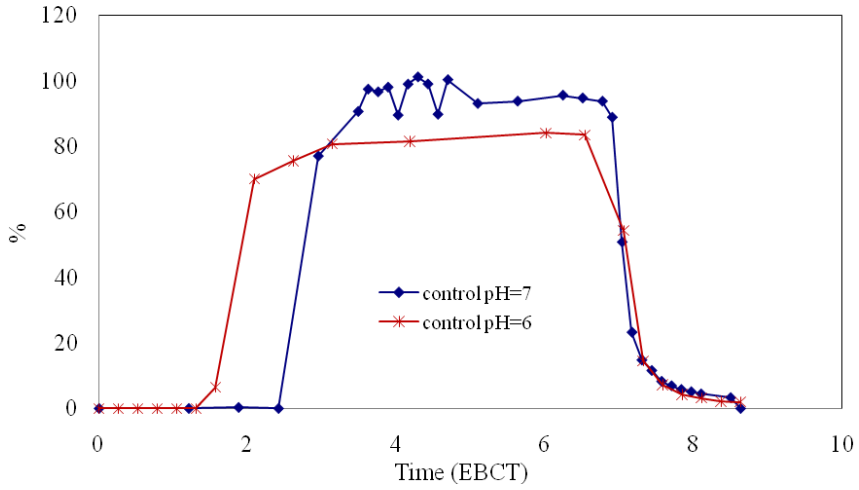

Fi g. 4.10 – As(V) breakthrough curves on iron oxide-coated sand at pH 6.0 and 7.0.

Figures 4.10 shows the breakthroughs of arsenate (As(V)) on iron oxide-coated sand obtained at pH 6.0 and 7.0. For pH 7.0, arsenate penetrated the column after 2.5 EBCT.

This means that about 1.5 EBCT volume of 20 ppm arsenate could be removed before the sand bed was penetrated. For removing 20 ppb level arsenate, this could be translated into a removing capacity for1500 EBCT of polluted water, which is quite significant. When pH was lowered from 7.0 to 6.0, the breakthrough occurred significantly earlier. The plateau concentration for pH 6.0 was lower than 7.0, suggesting that more As(V) was precipitated at pH 6.0. Overall the result shows that at neutral pH, the *in situ* produced iron oxide coating can treat significant amount of arsenate-contaminated water before capacity regeneration is required. Operating at a higher pH might further increase the removal capacity.

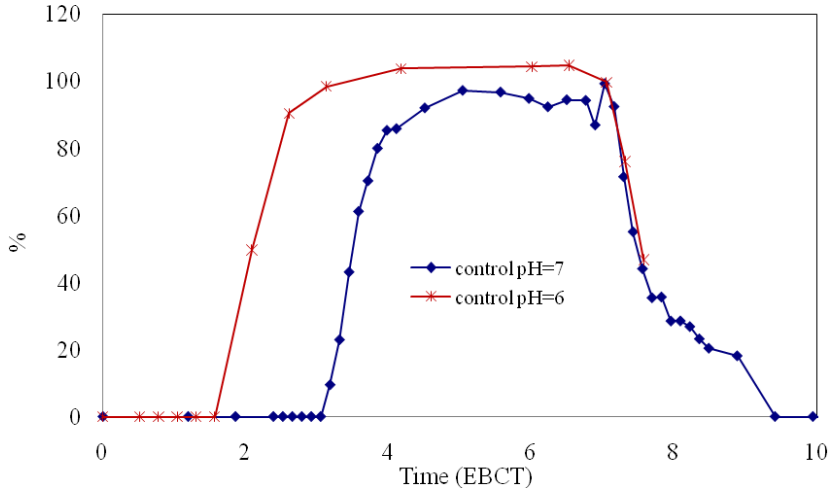

Fig. 4.11 – As(III) breakthrough curves on iron oxide-coated sand at pH 6.0 and 7.0.

Figures 4.11 shows the breakthroughs of arsenite (As(III)) on iron oxide-coated sand conducted at pH 6.0 and 7.0. For pH 7.0, arsenate penetrated the column after 3.2 EBCT.

This means that about 2.2 EBCT volume of 20 ppm arsenite could be removed before the sand bed was penetrated. For removing 20 ppb level arsenate, this could be translated into a removing capacity for 2200 EBCT of polluted water. When pH was lower from 7.0 to 6.0, the breakthrough occurred significantly earlier. The result shows that at neutral pH, the *in situ* produced iron oxide coating can treat significant amount of arsenite-contaminated water before regeneration of capacity is required. Overall, the iron oxide coating can more effectively remove arsenite than arsenate.

Comparison between As(III) and As(V) breakthrough pattern shows that As(III) has a more significant tailing than As(V). This suggest that adsorption of As(III) on iron oxide is more reversible than that of As(V).

4.3.2 Effect of previous breakthrough test on new test

Immediately after running the first breakthrough curve test at pH 7.0, a second breakthrough curve test was performed under the same condition. Overall, the iron-oxide-coated sand bed still demonstrates some but generally lower capacity for additional arsenic removal. The extended tailing suggests that the removal was more due to reversible adsorption than irreversible precipitation (i.e., chemisorptions). Note that this is done without placing a new iron oxide coating on sand, so the result should not be taken to represent the treating capacity after regeneration.

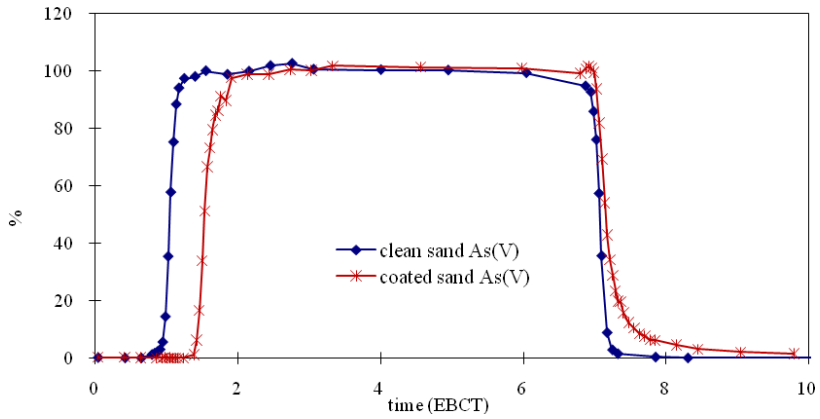

Fig. 4.12 – As(V) breakthrough curves on clean sand and iron oxide-coated sand at pH 7.0.

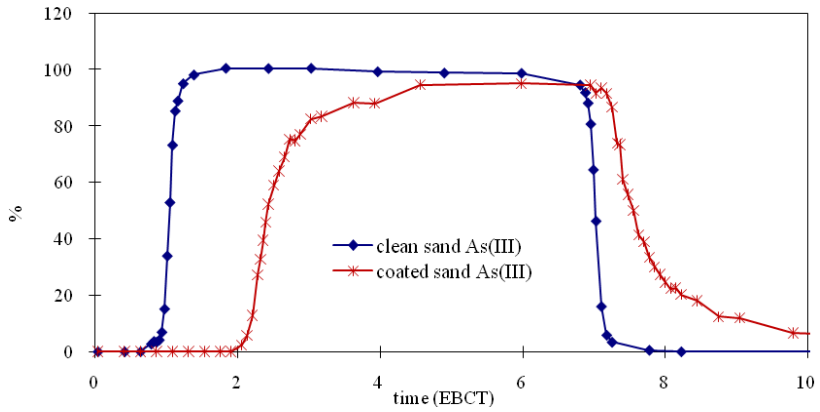

Fig. 4.13 –As(III) breakthrough curves on clean sand and iron oxide-coated sand at pH 7.0.

4.4 Modeling and parameter estimation

The transport parameters, such as dispersion coefficient *D*, distribution coefficient of adsorption K_d, can be obtained by using the equilibrium or non-equilibrium models to fit

the breakthrough curves. Software CXTFIT version 2.1 (Toride et al., 1999) was used to estimate the parameters of column experiments.

The convection-dispersion equation (CDE) for one-dimensional transport of reactive solutes, subject to advection, dispersion, linear equilibrium adsorption, and first-order degradation, in a homogeneous porous media, is written as:

$$R\frac{\partial C}{\partial t} = D\frac{\partial^2 C}{\partial z^2} - v_p\frac{\partial C}{\partial z} - \mu C \qquad \text{Eq.1}$$

where C is the resident concentration in the liquid phase (ML^{-3}); t is time (T); z is the vertical dimension of flow (L); v_p is the average pore velocity (LT^{-1}); D is the longitudinal dispersion coefficient (L^2T^{-1}); μ is an overall first-order decay coefficient including filtration (T^{-1}); and R is the retardation factor due to adsorption (dimensionless).

In addition,

$$R = 1 + \frac{\rho_b K_d}{\theta},$$

where ρ_b is the soil bulk density (ML^{-3}); θ is the volumetric water content (dimensionless); and K_d is the distribution coefficient of linear adsorption (L^3/M) describing the adsorption equilibrium relationship between the liquid and the sorbed phases.

4.4.1 Chloride pulse tracer test

Column breakthrough test using Cl^- as a conservative tracer is simulated by equilibrium model (setting R=1 and μ=0) to estimate v_p and D, by an optimization

routine that minimizes the error between model and experimental values. Fig. 4.14 shows the observed and model simulated breakthrough curves of Cl^- on clean sand at pH 6. The result indicates that the equilibrium model fits the transport processes of the non-reactive tracer in the homogeneous short column very well. The dispersion coefficient D can be determined as 12.22 cm^2/hr, and [11.14, 13.30] cm^2/hr with 95% confidence limits. The pore velocity v_p is 173 cm/hr.

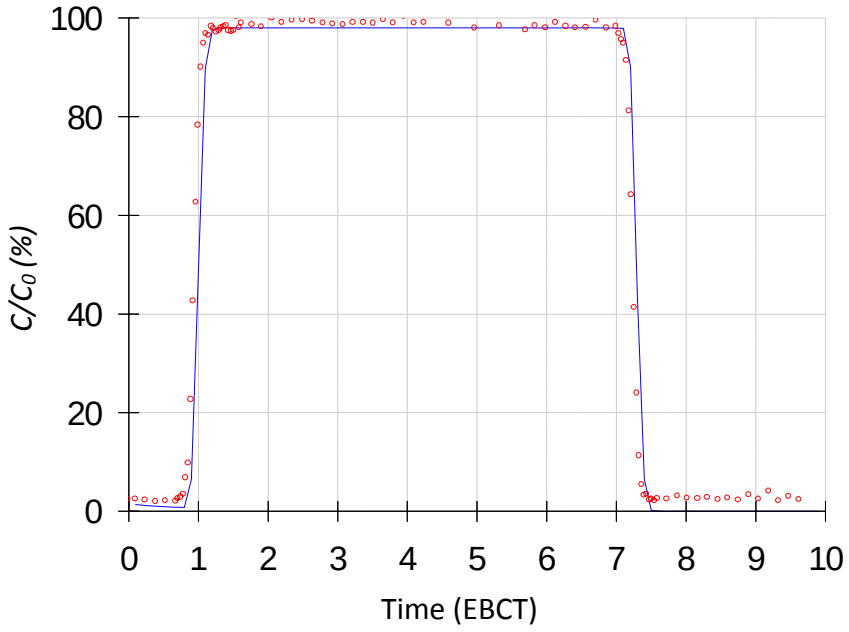

Fig. 4.14 – Simulation of Cl^- breakthrough curves using equilibrium model.

Table 4.1 lists the v_p and D values for each breakthrough experiment, calculated by CXTFIT equilibrium model.

Table 4.1 – Parameter estimation using CXTFIT equilibrium model

Breakthrough experiment	Pore velocity v_p (cm/hr)	Dispersion coefficient D (cm^2/hr)
Fe^{2+} on clean sand at pH=6.0	173	12.22±1.08
Fe^{2+} on coated sand at pH=6.0	142	15.94±1.94
Fe^{2+} on clean sand at pH=7.0	179	9.65±4.09
Fe^{2+} on coated sand at pH=7.0	167	8.27±1.34
As(V) on clean sand at pH=7.0	179	11.87±2.46
As(V) on coated sand at pH=7.0	178	13.33±5.75
As(III) on clean sand at pH=7.0	181	13.24±1.28
As(III) on coated sand at pH=7.0	176	10.54±1.89

4.4.2 Fe^{2+} and arsenic adsorption

The non-equilibrium model needs to be applied if the equilibrium model could not provide good fitting results. Fig. 4.15 shows that the non-equilibrium model fits much better than the equilibrium model for Fe^{2+} breakthrough curve on clean sand at pH 6.0.

In the two-region physical non-equilibrium model, we have to estimate β and ω, both of which are dimensionless variables for partitioning in non-equilibrium transport models. The v_p and D values obtained from the previous tracer breakthrough curve are used as fixed parameters.

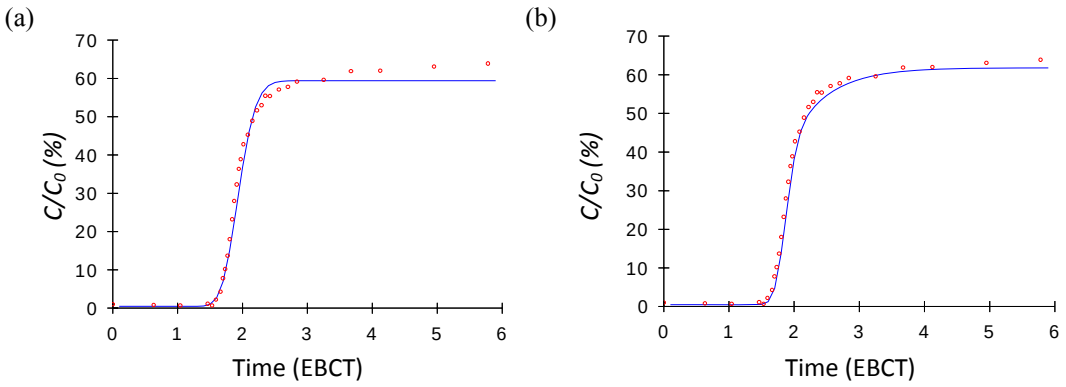

Fig. 4.15 – Simulation of Fe^{2+} breakthrough curves on clean sand at pH 6.0 using (a) equilibrium model and (b) non-equilibrium model.

The retardation factor R, distribution coefficient K_d, dimensionless variables β and ω values for each breakthrough experiment are listed in Table 4.2.

Table 4.2 – Parameter estimation using CXTFIT non-equilibrium model

	R (-)	β (-)	ω (-)	K_d (cm^3/g)
Fe^{2+} on clean sand at pH=6.0	1.72	0.8701	0.8456	0.101
Fe^{2+} on coated sand at pH=6.0	1.39	0.8770	0.1825	0.054
Fe^{2+} on clean sand at pH=7.0	2.34	0.0001	102.1	0.187
Fe^{2+} on coated sand at pH=7.0	3.40	0.0002	747.8	0.334
As(V) on clean sand at pH=7.0	1.05	0.9976	415.3	0.007
As(V) on coated sand at pH=7.0	1.59	0.9637	0.1129	0.082
As(III) on clean sand at pH=7.0	1.04	0.1907	1901	0.006
As(III) on coated sand at pH=7.0	2.58	0.9015	0.4516	0.220

4.5 Implication of the technique

The bench-scale column experiments have demonstrated the feasibility of the sequential injections of ferrous iron solution and hypochlorite solution for *in situ* generating an iron oxide coating on sand surface. Through managing factors such as pH, injection rate, and duration of each injection, it is possible to control precipitation of iron oxide at a certain distance from the inlet zone. Clogging of sand media that could be the major technical obstacle has been overcome through the insert of a water buffer between ferrous iron and oxidant plume. The arsenic removing capability of the resulting iron oxide coating was also demonstrated.

The *in situ* iron oxide emplacement technique we demonstrated could be developed into a cost-effective solution for treating arsenic-contaminated groundwater. For the purpose, we can inject preconditioned reagent solutions into an aquifer through a drinking water well and create a large zone of iron oxide-enriched soil media that can serve as a reactive barrier surrounding the well for removing arsenic and other pollutants. Compared to current practice of excavate-and-fill technique, our technique has clear advantages. First, it avoids the high cost associated with excavation. The practicability of excavate-and-fill technique is often limited by the engineering capability of depth excavation. Creating a 100 ft-deep reactive barrier using excavate-and-fill technique could be a significant challenge. In many occasions, geologic conditions could become an insurmountable constrain. For our *in situ* emplacement technique, depth is not a major concern. Second, our *in situ* technique can regenerate the reactive material much more easily than conventional excavate-and-fill technique.

In many regions of the US and around the world, many rural communities use arsenic-contaminated groundwater as their drinking water sources. Many of them lack economic viability and technical expertise to employ a costly and complicated method for arsenic treatment. The *in situ* technique could overcome this obstacle and provide a viable solution to these communities and require only limited initial capital expense and a little technical knowhow to install, operate and maintain our *in situ* treatment system. For example, by our calculation, an iron oxide-coated zone measuring 10 m in diameter and 10 m in depth surrounding a drinking well could treat over 2 million cubic meter of groundwater contaminated with 20 ppb arsenite before it needs regeneration. We estimate that 5,000 kg of ferrous salt would be sufficient for the purpose. The chemical cost can be limited to within $2,000, which translates into 0.001 dollar per cubic meter treated water. For a single household, a much smaller size system will be sufficient.

Furthermore, the *in situ* iron oxide coating technique could be used in many other applications. For example, the technique can be used to construct a reactive filter in the form of an above-ground reactor for removing heavy metals such as selenium and mercury from various industrial wastewaters. The method can also be used to create large scale subsurface reactive barrier as a remediation to many toxic metal-contaminated sites. For example, the technique could be used in many DoE contaminated sites to contain uranium plume.

This study only represents a proof of the concept. More studies are needed to further develop the technique. For example, we will like to test in the future if dissolved oxygen can replace hypochlorite as the oxidant. Hypochlorite could be a concern in a real

application. We also like to know if arsenic removed could be remobilized or be permanently encapsulated by a new layer of iron oxide through regeneration process. Redissolution and leaching of iron from the coated-sand media could be another concern. Field trials should be carried out at different sites and with different operation conditions.

5. CONCLUSIONS

In this study, we developed a novel technique that can *in situ* emplace iron oxides onto sand grain surfaces of porous media under mild chemical and temperature conditions. The technique involves sequential injections of a preconditioned ferrous iron solution and an oxidant solution and employs natural convective-diffusive transport of the two reagents in porous media to create an overlapped reaction zone where ferrous iron is oxidized and precipitated on the sand grain surface. We demonstrate through bench-scale column tests the feasibility of using this technique to create a large-scale iron oxide-enriched reactive barrier in subsurface environment for *in situ* removal of arsenic. A sand filter with fresh iron oxide coating could treat thousands of pore volume of water contaminated with dozens of ppb arsenic before it needs regeneration. The chemical cost will be less than \$0.01 per m^3 treated water. Modeling of arsenic breakthrough suggests that both reversible adsorption and irreversible precipitation are responsible for reduction of arsenic in the water. Unlike conventional excavated-and-filled permeable reactive barriers, the treatment capacity of our *in situ* created barrier can be *in situ* regenerated and replenished with a fresh coating.

REFERENCES

Aguilar, J., Dorronsoro, C., Fernandez, E., Fernandez, J., Garcia, I., Martin, F., Sierra, M., Simon, M., 2007. Remediation of As-contaminated soils in the Guadiamar river basin (SW, Spain). Water Air Soil Pollut. 180 (1-4), 109-118.

Benjamin, M.M., Chang, Y.J., Li, C.W., Korshin, G.V., 1993. NOM adsorption onto iron-oxide-coated sand. AWWA Research Foundation, Denver, CO.

Bose, P., Sharma, A., 2002. Role of iron in controlling speciation and mobilization of arsenic in subsurface environment. Water Res. 36 (19), 4916-4926.

Breeuwsm.A, Lyklema, J., 1973. Physical and chemical adsorption of ions in electrical double-layer on hematite (alpha-Fe2O3). J. Colloid Interface Sci. 43 (2), 437-448.

Chang, Y.Y., Song, K.H., Yang, J.K., 2008. Removal of As(III) in a column reactor packed with iron-coated sand and manganese-coated sand. J. Hazard. Mater. 150 (3), 565-572.

Chen, W.F., Parette, R., Zou, J.Y., Cannon, F.S., Dempsey, B.A., 2007. Arsenic removal by iron-modified activated carbon. Water Res. 41 (9), 1851-1858.

Cherry, J.A., Shaikh, A.U., Tallman, D.E., Nicholson, R.V., 1979. Arsenic species as an indicator of redox conditions in groundwater. J. Hydrol. 43 (1-4), 373-392.

Ferguson, J.F., Gavis, J., 1972. Review of arsenic cycle in natural waters. Water Res. 6 (11), 1259-1274.

Genz, A., Baumgarten, B., Goernitz, M., Jekel, M., 2008. NOM removal by adsorption onto granular ferric hydroxide: equilibrium, kinetics, filter and regeneration studies. Water Res. 42 (1-2), 238-248.

Hug, S.J., Leupin, O., 2003. Iron-catalyzed oxidation of arsenic(III) by oxygen and by hydrogen peroxide: pH-dependent formation of oxidants in the Fenton reaction. Environ. Sci. Technol. 37 (12), 2734-2742.

Hutton, M., 1987. Human health concerns of lead, mercury, cadmium and arsenic. In: Hutchinson, T.C., Meema, K.M., (Eds.), Lead, Mercury, Cadmium and Arsenic in the Environment, John Wiley and Sons, New York, pp. 53-68.

Jain, A., Raven, K.P., Loeppert, R.H., 1999. Arsenite and arsenate adsorption on ferrihydrite: surface charge reduction and net OH- release stoichiometry. Environ. Sci. Technol. 33 (8), 1179-1184.

Joshi, A., Chaudhuri, M., 1996. Removal of arsenic from ground water by iron oxide-coated sand. J. Environ. Eng-ASCE. 122 (8), 769-771.

Kanel, S.R., Greneche, J.M., Choi, H., 2006. Arsenic(V) removal from groundwater using nano scale zero-valent iron as a colloidal reactive barrier material. Environ. Sci. Technol. 40 (6), 2045-2050.

Kim, M.J., Nriagu, J., 2000. Oxidation of arsenite in groundwater using ozone and oxygen. Sci. Total Environ. 247 (1), 71-79.

Ko, L., Davis, A.P., Kim, J.Y., Kim, K.W., 2007. Arsenic removal by a colloidal iron oxide-coated sand. J. Environ. Eng-ASCE. 133 (9), 891-898.

Kundu, S., Gupta, A.K., 2007. As(III) removal from aqueous medium in fixed bed using iron oxide-coated cement (IOCC): Experimental and modeling studies. Chem. Eng. J. 129 (1-3), 123-131.

Lenoble, W., Laclautre, C., Deluchat, W., Serpaud, B., Bollinger, J.C., 2005. Arsenic removal by adsorption on iron(III) phosphate. J. Hazard. Mater. 123 (1-3), 262-268.

Lin, Z., and Puls, R.W., 2003. Potential indicators for the assessment of arsenic natural attenuation in the subsurface. Adv. Environ. Res. 7(4), 825-834.

Miretzky, P., Cirelli, A.F., 2010. Remediation of arsenic-contaminated soils by iron amendments: a review. Crit. Rev. Environ. Sci. Technol. 40 (2), 93-115.

Pedersen, H.D., Postma, D., Jakobsen, R., 2006. Release of arsenic associated with the reduction and transformation of iron oxides. Geochim. Cosmochim. Acta 70 (16), 4116-4129.

Pokhrel, D., Viraraghavan, T., 2008. Arsenic removal from an aqueous solution by modified A-niger biomass: batch kinetic and isotherm studies. J. Hazard. Mater. 150 (3), 818-825.

Raven, K.P., Jain, A., Loeppert, R.H., 1998. Arsenite and arsenate adsorption on ferrihydrite: kinetics, equilibrium, and adsorption envelopes. Environ. Sci. Technol. 32 (3), 344-349.

Regner, G., Court, M., Kreig, K., 2004. Health effects and occurrence of arsenic in Texas' water supplies. Texas Commission on Environmental Quality.

Schwertmann, U., Cornell, R., 2000. Iron oxides in the laboratory: preparation and characterization. VCH, Weinheim.

Smedley, P.L., Kinniburgh, D.G., 2002. A review of the source, behaviour and distribution of arsenic in natural waters. Appl. Geochem. 17 (5), 517-568.

Thirunavukkarasu, O.S., Viraraghavan, T., Subramanian, K.S., 2003. Arsenic removal from drinking water using iron oxide-coated sand. Water Air Soil Pollut. 142 (1-4), 95-111.

Toride, N., Leij, F. J., van Genuchten, M. T., 1999. The CXTFIT code for estimating transport parameters from laboratory or field tracer experiments. Version 2.1, Research Report No. 137, U. S. Salinity Laboratory, USDA, Riverside, CA.

Vaishya, R.C., Gupta, S.K., 2003. Arsenic removal from groundwater by iron impregnated sand. J. Environ. Eng-ASCE. 129 (1), 89-92.

Welch, A.H., Lico, M.S., Hughes, J.L., 1988. Arsenic in ground-water of the Western United-States. Ground Water 26 (3), 333-347.

Westall, J.C., Zachary, J.L., Morel, F.M.M., 1976. MINEQL: a computer program for the calculation of chemical equilibrium composition of aqueous systems. Technical Note 18, Ralph M. Parsons Laboratory, MIT, Cambridge, MA

WHO, 2006. Arsenic in the drinking water. Fact Sheet 210, Geneva: World Health Organization.

Ying, X., Axe, L., 2005. Synthesis and characterization of iron oxide-coated silica and its effect on metal adsorption. J. Colloid Interface Sci. 282 (1), 11-19.

Zeng, L., 2003. A method for preparing silica-containing iron(III) oxide adsorbents for arsenic removal. Water Res. 37 (18), 4351-4358.

VITA

Name: Hongxu Yu

Address: Department of Biological & Agricultural Engineering,
303E Scoates Hall, 2117 TAMU,
College Station, TX 77843

Email Address: yuhongxu@gmail.com

Education: B.A., Environmental Engineering, Tsinghua University, 2004
M.S., Civil Engineering, Tsinghua University, 2007
M.S., Biological and Agricultural Engineering, Texas A&M University, 2010